Characterization of line-of-sight and non-line-of-sight pseudo-range and pseudo-range rate multipath errors in an urban environment

Eustachio Roberto Matera, Olivier Julien, Axel Garcia-Pena, Bertrand Ekambi
Ecole Nationale de l'Aviation Civile (ENAC), Toulouse, France

Extended Abstract

Nowadays, navigation systems integrating at least inertial measurement unit (IMU) and GNSS signal processing units are becoming the fundamental baseline platform for mass-market user devices. Such platforms aim at combining reasonably low-cost hardware with the provision of the highest possible positioning accuracy, availability and reliability.

Although IMU specifically complements the weak points of the GNSS systems, low availability in urban/indoor scenarios as well as poor pseudo-range measurement performance in urban canyons due to multipath phenomenon, the hybrid system will still rely on GNSS measurements for correcting IMU increasing-in-time bias errors. Therefore, in order to obtain an optimal and reliable position estimate, it is necessary to have access to an accurate assessment of the GNSS measurements even in difficult environments; in other words, it is necessary to model accurately the pseudo-range and pseudo-range rate error distribution. The objective of this work is thus to provide a highly realistic model of the GNSS measurement error in an urban and sub-urban environment, in particular regarding the pseudo-range and pseudo-range rate measurements. More specifically, this article will provide a methodology to characterize the pseudo-range and pseudo-range rate measurement errors due to multipath for a GNSS receiver in a car. The innovations of the work consist in trying to discriminate the measurements' error distribution between the Line-of-Sight (LOS) and Non Line-of-Sight (NLOS) situations, and to compare the results according to different signals in the L1 band.

The methodology followed to characterize the multipath-induced error consist in the following five steps:

1) Data Collection
2) Errors isolation from pseudo-range and pseudo-range rates from a low-cost receiver

3) Errors isolation from pseudo-range and pseudo-range rates from reference station receiver
4) Multipath error isolation
5) LOS and NLOS Multipath error characterization

1) Data Collection: The data to be analysed is collected by using a receiver (a uBlox M8T in the paper) installed on the roof of the ENAC test vehicle which will be driven within the representative area of interest (Toulouse urban area in the paper). Data from a fish-eye camera and a NovAtel SPAN receiver is also collected at the same time. The fish-eye camera is mounted on top of the test vehicle up-facing and is used to record images of the car's environment: the images will be used to determine if the given satellite is in LOS or in NLOS signal reception conditions. The NovAtel SPAN receiver is used to obtain a very precise trajectory of the car during the data collection.

2) Errors isolation from low-cost receiver: The collected NovAtel SPAN measurements are then used to compute a very accurate vehicle position (typcically within a few centimeters), which can be extrapolated to the test receiver antenna using the known lever-arm between the two systems. This provides a very accurate estimate of the test receiver's antenna location. Based on the known location and speed of the visible GNSS satellites, it is thus possible to compute the true distance and velocity between the test receiver antenna and each individual satellite. In this way, it is possible to remove from the pseudo-range and pseudo-range rate measurements obtained by the test receiver these estimated range and range rates. The resulting values only contain the measurement errors (dominated by the atmospheric errors, noise and multipath, especially in the urban environment), satellite and receiver clock offsets (or drift),.

3) Errors isolation from reference station receiver: The same process is used to estimate the closest reference station "range free" pseudo-range and pseudo-range rate, knowing exactly the position of the reference station. The resulting measurements are constituted of the same errors as mentioned before, but, with a smaller order of magnitude regarding noise and multipath errors, due to the high quality of the receiver and the position of the reference station (much less multipath).

4) Multipath Error isolation: Assuming that the refence station is sufficiently close to the location of the test receiver during the data collection, it can be assumed that the ionospheric and tropospheric delays, which are space correlated, are more or less the same at the test receiver and reference station. Thus, applying again a difference between the "range free" component obtained in the 2 previous steps, one can obtain the removal of the atmospheric

errors and satellite clock and ephemeris errors terms. The obtained measurements now consist only of the difference between the test receiver and reference station receiver clock terms, the differenced multipath error and differenced noise. Assuming that the multipath and thermal noise errors experienced by the test receiver are much greater than those experienced by the reference receiver, the measurements can now be considered to be dominated by the test receiver multipath and noise errors on one side, and the reference and test receiver clocks on the other side. Finally, the test receiver's multipath and noise errors are isolated with the respect to the receiver clock error applying a clock removal mechanism based on clock estimation and low pass filter.

5) LOS and NLOS Multipath error characterization: Once the multipath and noise error is isolated for each satellite, it is then interesting to classify the errors according to the reception condition, and more specifically if the receiver was in direct LOS or NLOS reception for a given satellite at a given time. As mentioned earlier, this classification can made by using the images recorder by the fish-eye camera: by using an image processing algorithm (determining the obstacles and the portion of the sky that is visible) and knowing the position of the satellites, the satellites can be classified into LOS and NLOS depending on whether an obstacle is determined to be between the geometrical straight line between the receiver and the transmitting satellite. Note that to do so, the attitude of the vehicle has to be known very accurately, which is possible thanks to the outputs of the NovAtel SPAN receiver. The estimated test receiver's multipath and noise error characterization can then be even further analysed as a function as a function of the estimated received C/N_0 and/or elevation angle.

Some early results are shown in 4 figures below. The results are obtained using the configuration presented in Table 1 .

Sample frequency data (Hz):	1
Sample frequency pictures (Hz):	1
Clock bias filter type	Bessel
Clock bias filter order	first order
Clock bias filter cutting frequency (Hz)	0.1
Duration of the used measurements (min):	25
Satellite Constellations	GPS constellation

Table 1 - Dataset configuration

These figure describe the uBlox M8T's estimated multipath and noise error probability density function for LOS cases (Figure 1, Figure 2) and NLOS cases (Figure 3, Figure 4), for signals with a receiver C/N0 between 30 and 40 dB-Hz (Left) and between 40 and 50 dB-Hz.

Future work will consist in building a position estimator that can take full advantage of this type of fine measurement characterization. Two possible approaches will be followed: (1) the use of a LOS/NLOS situation detector that will allow to use the appropriate measurement errors' distribution, that will be approximated by a Gaussian distribution and thus will be adapted to typical estimation techniques such as Extended Kalman Filter, or (2) to try to directly use the more complex measurement error model distribution of measurements in a more innovative navigation filter.

The article will be organized as follows:

- Section 1 will introduce the context and provide general concepts related to GNSS positioning in urban environment.
- Section 2 will describe the mechanism to isolate the test receiver's multipath and noise errors.
- Section 3 will present the LOS/NLOS situation detector based on the fish-eye camera.
- Section 4 will present the experimental set up and the proposed models for LOS, NLOS and all measurements.
- Finally, conclusions and future works will be derived in Section 5.

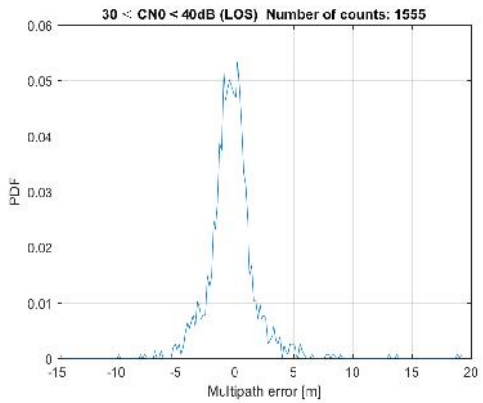

Figure 1 - Multipath error Pobability Density Function between 30 dB and 40 dB of C/N0 , obtained with 1555 number of samples of multipath errors from LOS satellites

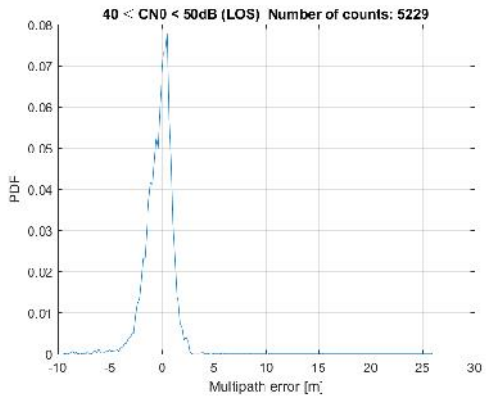

Figure 2 -Multipath error Pobability Density Function between 40 dB and 50 dB of C/N0 , obtained with 5229 number of samples of multipath errors from LOS satellites

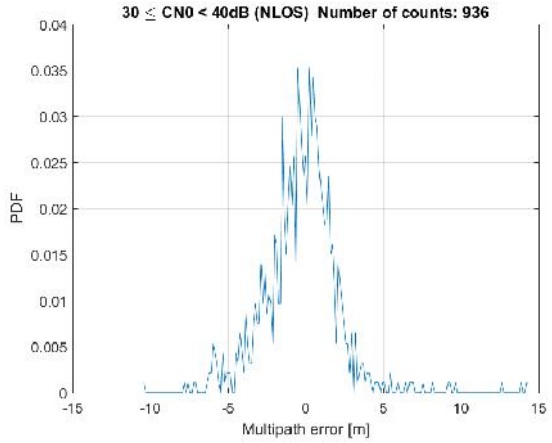

Figure 3 - Multipath error Pobability Density Function between 30 dB and 40 dB of C/N0 , obtained with 936 number of samples of multipath errors from NLOS satellites

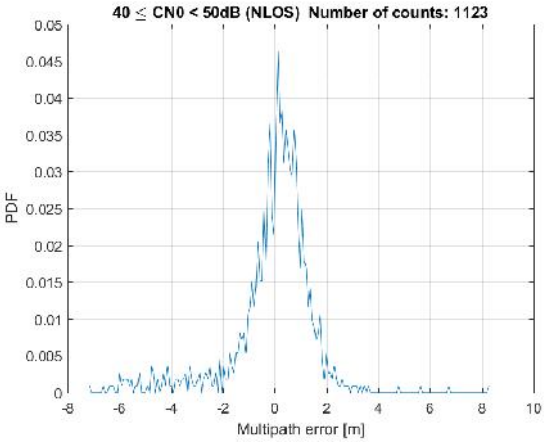

Figure 4 - Multipath error Pobability Density Function between 30 dB and 40 dB of C/N0 , obtained with 1123 number of samples of multipath errors from NLOS satellites